IEICE TRANSACTIONS

on Fundamentals of Electronics, Communications and Computer Sciences

DOI:10.1587/transfun.2024EAL2036

Publicized:2024/08/23

This advance publication article will be replaced by the finalized version after proofreading.

A PUBLICATION OF THE ENGINEERING SCIENCES SOCIETY
The Institute of Electronics, Information and Communication Engineers
Kikai-Shinko-Kaikan Bldg., 5-8, Shibakoen 3 chome, Minato-ku, TOKYO, 105-0011 JAPAN

LETTER

A scalable frequency estimation method based on multi-point interpolation of trigonometric functions

Li Cheng[†a)], ***Member and*** **Huaixing Wang**[†], ***Nonmember***

SUMMARY Interpolation-based frequency estimation methods can be used to improve the frequency estimation accuracy of discrete Fourier transform (DFT) methods for complex exponential or real sinusoidal signals. However, traditional interpolation methods first need to search for the maximum spectral line and its adjacent spectral lines in order to interpolate the frequency estimate. This type of method has a low degree of flexibility and does not make full use of the effective information in the frequency domain. In order to solve this problem, this paper proposes a scalable frequency estimation method based on the multiple point interpolation of trigonometry, eliminating the need to find the peak of the spectrum and using multiple point spectral information to improve the frequency estimation accuracy. This paper first derives the formula for frequency estimation of complex sinusoidal signals using multiple spectral lines by using the trigonometric constant equation, then analyses the effects of frequency interval and number of selected frequency points on the frequency estimation error, and finally verifies the estimation performance of the proposed estimator against competing estimators by simulation. Simulation results show that the root mean square error (RMSE) of the estimator is closer to Cramer-Rao Lower Bound (CRLB) than those of the competing estimators over the whole effective signal-to-noise ratio (SNR) range.

key words: *DFT interpolation, frequency estimation, RMSE, trigonometric function*

1. Introduction

Frequency estimation is widely used for signal detection and Doppler tracking [1] in many engineering applications, such as music [2], radar [3], sonar [4] and satellite navigation [5], etc. Commonly used methods for estimating frequency include time domain method [2], frequency domain method [6] and joint time-frequency method [7]. The frequency estimation method based on discrete Fourier transform (DFT) takes advantage of the efficient fast Fourier transform (FFT) algorithm. The method is generally divided into two steps: the first step is a coarse estimation of frequency using the DFT coefficient with the highest magnitude, and the second step tries to refine the coarse frequency. In the fine-tuning step, traditional methods often use the peak magnitude of DFT and its nearest neighbors to design a suitable Fourier interpolation algorithms.

In general, the interpolated DFT method can be divided into the direct methods, and the iterative methods. The direct method is obtained by taking the Fourier transform function of the sequence and expanding it in a Taylor series expansion [8]. And its accuracy is strongly correlated with the error in the estimation of the peak frequency [9]. In order to reduce the dependence on frequency offset, Liao [10] derived a new set of simple analytical unbiased estimators. Then he showed that correcting a phase term before interpolation can reduce the estimation bias [11]. In 2020, Shigeru Ando [6] proposed a frequency-domain Prony method based on the AR model expressed by Fourier coefficients, which can estimate frequencies for both isolated and indecomposable sinusoids, with the advantages of anti-noise and high statistical efficiency. Meanwhile, the iterative methods have been proposed to further improve the accuracy of frequency estimation. Aboutanios and Mulgrew [12] proposed a method using two DFT coefficients with two iterations, resulting in asymptotic variance of 1.0147 times the Cramer-Rao Lower Bound (CRLB). However, the iterative approach is computationally expensive and not suitable for real-time processing of signals. Therefore, a noniterative two-point interpolation estimator using sinc function fitting was proposed, the estimated standard deviation can be reduced to 1.0073 times of the CRLB [13].

In recent years, three or more DFT coefficients, including the maximum magnitude, have been used to improve the performance of estimation. Candan theoretically derived and extended the empirically based estimator [9] to form a new estimator using three spectral lines [8], followed by an unbiased estimator [14]. Mou [15] used three-point interpolation with an iterative approach to achieve multiple frequency estimation, which performs close to CRLB over a wide signal-to-noise ratio (SNR) range. Orguner [16] proposed the best linear unbiased estimation criterion by merging multiple DFT samples, achieving high frequency estimation accuracy with high SNR. Macleod [17] improved performance by performing frequency estimation with five-point DFT samples, but the method requires samples centered on the peak location.

To improve estimation performance without increasing algorithm complexity, this paper proposes a scalable frequency estimator based on multi-point interpolation of trigonometric functions. The frequency interval of the method is arbitrary, and the method can be flexibly extended to further improve frequency estimation accuracy using multi-point interpolation.

† The author are with Dept. of Physics, Mechanical and Electrical Engineering, Hubei University of Education, Wuhan 430205, China.
a) E-mail: lcheng@hue.edu.cn.

2. Signal model and problem formulation

A complex exponential signal embedded in additive white Gaussian noise (AWGN) can be modeled as:

$$y(t) = x(t) + r(t) = Ae^{j(2\pi f_0 t + \theta_0)} + r(t) \quad (1)$$

The discrete form obtained by sampling the continuous time signal $y[n]$ can be expressed as:

$$y[n] = Ae^{j(2\pi n f_0/f_s + \theta_0)} + r[n], n = 0,1,\cdots,N-1 \quad (2)$$

where A, f_0, and θ_0 are the amplitude, frequency, and initial phase of the complex sinusoidal signal respectively. f_s is the sampling frequency, and N is the observation length. $r[n]$ is complex and zero mean AWGN with variance σ^2. The SNR is defined as $SNR = A^2/\sigma^2$. Our objective is the estimation of the sinusoidal signal frequency in the presence of the unknown amplitude and initial phase by a block of N samples.

In the absence of noise, the truncated sinusoidal signal $x(t)$ is equivalent to performing a rectangular window of the samples. If $\mathrm{sinc}(x)$ function is defined as $\mathrm{sinc}(x) = \sin x/x$, the Fourier transform $F(f)$ of a complex sinusoid $x(t)$ is given by:

$$F(f) = \int_{-\frac{T}{2}}^{\frac{T}{2}} Ae^{j(2\pi f_0 t + \theta_0)} e^{-j2\pi f t}\, dt = ATe^{j\theta_0}\mathrm{sinc}(\pi T(f - f_0)) \quad (3)$$

where $T = N/f_s$ is the sampling duration of the input sinusoid. According to Eq. (4) the spectrum obtained from the Fourier transform of a complex exponential signal is a sinc function.

The Discrete Time Fourier Transform (DTFT) for a noiseless complex sinusoid is shown in Fig. 1, where the number of samples is N=16 and the normalized frequency is $F_0 = 0.025$. We assume that f_0 is normalized to the sampling rate f_s, which guaranties that $F_0 \in [-0.5, 0.5]$. Fig. 1 shows that by truncating the time domain signal, the spectrum of the sinusoid is no longer a single tone. It is expanded into a sinc-shaped narrowband signal, which appears as a spectrum leakage. The magenta star represents the complex sinusoidal DTFT peak. The blue dot represents the zero frequency of the signal and its magnitude is given by A_P. To the left of the blue dot, the red dots (A_{Li}) represent sampled magnitudes in the frequency domain with intervals of $-i\Delta f$ from the zero frequency, respectively, the cyan dots to the right (A_{Ri}) represent sampled magnitudes with intervals of $i\Delta f$ from the zero frequency. The magnitudes A_{Li}, A_P, and A_{Ri} can be calculated using the DTFT of the noisy observation. These magnitudes can be used to refine the frequency accuracy in the interpolated DFT method.

The CRLB of the frequency of a complex exponential signal embedded in noise was derived in [18]:

$$\sigma_f^2 = \frac{6f_s^2}{(2\pi)^2 N(N^2-1)SNR} \quad (4)$$

Where N, f_s, and SNR are the observation length, sampling frequency, and the SNR respectively. It can be seen from the equation that a larger observation window size or higher SNR improves the accuracy of the frequency estimation [19].

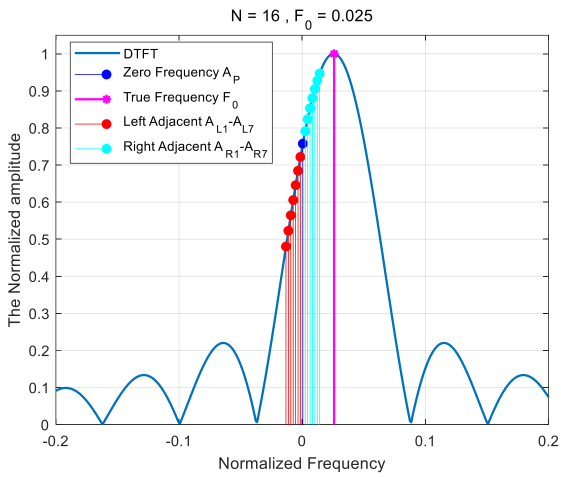

Fig. 1 The DTFT periodogram with zero frequency and multi-point interpolation.

3. Proposed estimator based on multi-point interpolation

The proposed method can use M odd DTFT points to interpolate for the location of the true frequency. In particular, the coefficients to the left and right of the zero frequency are A_{Li} and $A_{Ri}, i = 1,\cdots,\frac{M-1}{2}$. Intercepting a portion of a complex sinusoid for analysis, it is equivalent to adding a rectangular window to the signal. These frequency domain coefficients, A_P, A_{Li} and A_{Ri}, all lie on the sinc function curve. According to the identity of the trigonometric function, we have:

$$\sum_{i=1}^{\frac{M-1}{2}} \sin[\pi T(f_0 - i\Delta f)] + \sum_{i=1}^{\frac{M-1}{2}} \sin[\pi T(f_0 + i\Delta f)] = 2\sum_{i=1}^{\frac{M-1}{2}} \sin(\pi T f_0)\cos(\pi T i\Delta f) \quad (5)$$

where f_0 is the true frequency of the complex sinusoid. By substituting $\mathrm{sinc}(x) = \sin x/x$ into Eq. (5), we obtain:

$$\sum_{i=1}^{\frac{M-1}{2}} \mathrm{sinc}[\pi T(f_0 - i\Delta f)][\pi T(f_0 - i\Delta f)] + \sum_{i=1}^{\frac{M-1}{2}} \mathrm{sinc}[\pi T(f_0 + i\Delta f)][\pi T(f_0 + i\Delta f)] = \sum_{i=1}^{\frac{M-1}{2}} 2\mathrm{sinc}(\pi T f_0)(\pi T f_0)\cos(\pi T i\Delta f) \quad (6)$$

Define A_{Li}, A_P, and A_{Ri} as follows:

$$\begin{cases} A_{Li} = \mathrm{sinc}[\pi(f_0 - i\Delta f)T] \\ A_P = \mathrm{sinc}(\pi f_0 T) \\ A_{Ri} = \mathrm{sinc}[\pi(f_0 + i\Delta f)T] \end{cases} \quad (7)$$

Then, Eq. (6) can be written as:

$$\pi T\sum_{i=1}^{\frac{M-1}{2}} [A_{Li}(f_0 - i\Delta f) + A_{Ri}(f_0 + i\Delta f)] = 2\pi T\sum_{i=1}^{\frac{M-1}{2}} A_P f_0 \cos(\pi T i\Delta f) \quad (8)$$

We can drive the following equation for estimating of f_0:

$$\hat{f}_0 = \frac{\left[\sum_{i=1}^{\frac{M-1}{2}} iA_{Ri} - \sum_{i=1}^{\frac{M-1}{2}} iA_{Li}\right]\Delta f}{\sum_{i=1}^{\frac{M-1}{2}}(A_{Li} + A_{Ri}) - 2A_P\sum_{i=1}^{\frac{M-1}{2}}\cos(\pi T i\Delta f)} \quad (9)$$

From Eq. (9), the frequency estimation of the complex sinusoid is determined by A_{Li}, A_P, A_{Ri}, Δf, and M.

The proposed method differs from existing frequency domain estimation methods in the following ways: first, the zero frequency of the intercepted signal is found in the first step instead of searching for the DFT peak; second, the frequency domain DTFT coefficients are selected at frequency intervals of $\pm i\Delta f, i = 1,2,\cdots,\frac{M-1}{2}$ on the left and right sides of the zero frequency. These M coefficients correspond to the amplitudes A_{Li}, A_P, and A_{Ri}; Third, the frequency interval can be taken arbitrarily in the main lobe of the frequency spectrum. It can be flexibly adjusted for frequency estimation according to practical needs.

4. Parameter selection and analysis

Equation (9) shows that the accuracy of the frequency estimation is related to the frequency interval Δf and the selected coefficient M. Therefore, the effect of the frequency interval on the frequency estimation accuracy is analyzed by simulation experiments at different SNRs. In the experiment, the amplitude of the complex exponential signal A=1, θ_0 is a random initial phase uniformly distributed on [0,2π], and the noise is AWGN. The signal frequency f_0 is assumed to be 10 Hz. The number of signal sampling points N is 16 with a sampling frequency of 1 KHz.

Figure 2 shows the frequency bias of the algorithm proposed in this paper for different values of M without noise. The bias is the absolute value of the difference between the estimated frequency and the true frequency. It can be seen from the figure that when M=3, the bias decreases with increasing frequency interval, reaching a minimum at 45 Hz. The bias follows a similar pattern when M is equal to 5, 7 or 9. Extensive simulations show that the bias is minimal when $\Delta f = 2f_s/(MN)$.The bias is 0.008 Hz for M=9 and 0.05 Hz for M=3 when the frequency interval is 12.7 Hz. Frequency estimation accuracy improves by 84% when M=9 is selected. This is because, in the proposed method, the range of frequency intervals used $[-(M-1)\Delta f/2, (M-1)\Delta f/2]$ increases as M increases, which effectively improves the accuracy of frequency estimation.

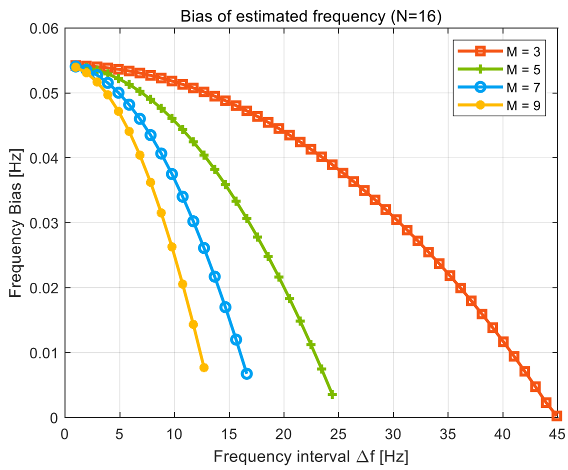

Fig. 2 Effect of different Δf and M on frequency bias without noise.

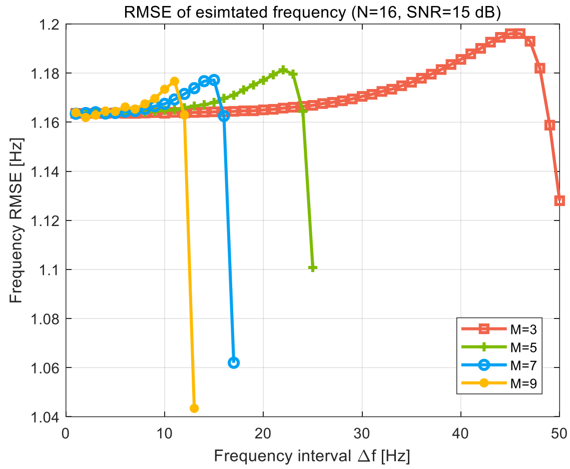

Fig. 3 Effect of different Δf and M on frequency RMSE at low SNR.

Figure 3 shows the results of the effect of Δf on the accuracy of the frequency estimation at an SNR of 15 dB. In the figure, the root mean square error (RMSE) is the square root of the mean of the squared errors of the estimated frequencies over the true frequencies of the sinusoid. The figure shows a significant increase in the frequency RMSE due to the increased noise compared to the noiseless case. In addition, at low SNR, the declining trend of the frequency RMSE is suppressed by the noise. The optimal Δf with M=3 increases slightly to around 50 Hz, while the estimators with M=5, 7, 9 have a better noise immunity and the optimal Δf remains essentially the same, reaching a minimum at $\Delta f = 2f_s/(MN)$. Selecting different M in the spectral line still follows the principle that the more frequency points selected, the better the anti-noise performance and frequency estimation accuracy. Therefore, it is advisable to use SNRs and frequency estimation error metrics when choosing frequency points and intervals in practice.

5. Simulation results and performance comparison

The performance of the proposal estimator is compared with the other conventional DFT interpolation estimators in this section. The competing estimators include the Candan estimator (CE) [8] and the Macleod estimator (ME) [17]. In the simulations, CE and ME (M=3) make use of the DFT peak and its two neighbors, while ME (M=5) is implemented using a five-sample interpolator. And the Δf of the proposed method is chosen following the optimum in Sect. 4.

First, the computational complexity of the different methods is compared. Since the traditional methods need to find the peak of the spectrum, they need to calculate the results of the DFT for all N points. In contrast, the proposed method only needs to compute the amplitude of the spectral lines around the zero frequency point using DTFT, thus greatly reducing the computational burden. This improvement will be significant when the frequency interval Δf is small, as the traditional methods have to improve the spectral density by zero padding.

Second, we evaluate and compare the effect of peak frequency estimation error on frequency estimating accuracy performance. In the simulation, the sampled sinusoidal sequence $f_0 = 10\text{Hz}$, $f_s = 1\text{KHz}$, *SNR*=15 dB and *N*=16. In the figures, the δ is defined as the frequency offset between the peak value and the real frequency f_0, normalized by the spectral line spacing, i.e., $\delta \in [-0.5, 0.5]$. For consistency, the zero-frequency location of the proposed method is set as the peak location of the other methods. And the Δf is set to 41.67Hz.

Figure 4 shows the RMSE performance for the different estimators at a low SNR. It can be seen that the frequency estimation errors of ME (*M*=3) and ME (*M*=5) gradually decrease with increasing $|\delta|$. Conversely, the estimating RMSEs of CE and the proposed estimator increase. The RMSE/CRLB of CE increases from 1.3 to 2, which is the highest RMSE, over the whole frequency offset range. In contrast, the proposed estimator only increases from 1.0 to 1.2, which is significantly better than CE. Fig.4 also shows that the proposed method achieves the CRLB over a wider range of δ. This indicates that its performance is less dependent on the frequency offset. Thus, our estimator outperforms the other two estimators at a low SNR.

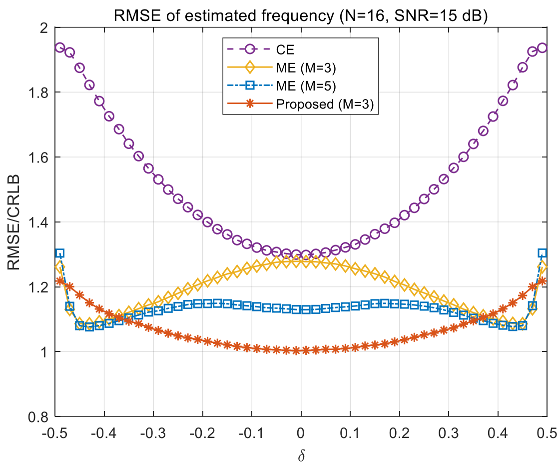

Fig. 4 RMSE comparison of frequency estimators at low SNR.

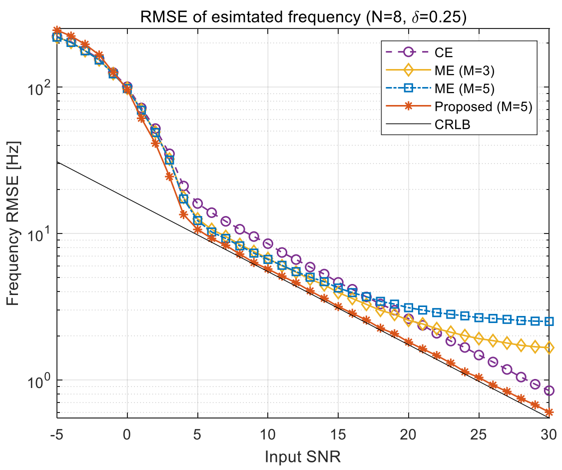

Fig. 5 The RMSE performance of the estimators versus SNR.

Third, the frequency estimation accuracy of estimators with different SNRs is evaluated and compared. Fig. 5 shows the frequency RMSE performance of the different estimators at a wide range of SNRs. In the experiment, *N*=8, $\delta = 0.25$ and a SNR ranging from -5 dB to 30 dB are used. *M*=5 and the optimal frequency interval 50 Hz is used in the proposed estimator. The figure shows that when the SNR is less than 5 dB, all algorithms deviate significantly from the CRLB. In the low SNR range, the ME with *M*=5 shows a slight performance improvement over *M*=3. However, both ME with *M*=5 and *M*=3 deviate significantly from the CRLB in the high SNR range. The CE performs worst in the low SNR range from 0 dB to 16 dB. However, it outperforms the ME above 20 dB. Over the whole range of SNRs, the RMSE performance of the proposed estimator is much closer to the CRLB than the others.

6. Conclusion

A scalable frequency estimator based on multi-point interpolation of trigonometric functions is proposed in this paper. The spectral lines used in this estimator don't have to be located next to the maximum magnitude. And the frequency interval can be taken to be arbitrary. The effects on the accuracy of frequency estimation of the frequency interval Δf and the selected coefficient M are analyzed. Simulation results show that the RMSE of the proposed estimator is closer to the CRLB than those of the competing estimators over the whole effective SNR range.

Acknowledgments

This work was supported in part by the Scientific Research Project of the Education Department of Hubei Province under grant D20223002, in part by the Scientific Research Foundation of Hubei University of Education for Talent Introduction under grant ESRC20220025, and in part by the teaching reform project X2023040, Hubei University of Education.

References

[1] L. Cheng, “An FLL structure based on a DFT interpolation discriminator for tracking weak GNSS signal,” IEICE Electronics Express, vol.21, no.7, pp.1-6, 2024.
[2] A. D. Cheveigne and H. Kawahara, "YIN, a fundamental frequency estimator for speech and music," J. Acoust. Soc. of America, vol. 111, no. 4, pp. 1917-1930, 2002.
[3] F. Engels, P. Heidenreich, A. M. Zoubir, F. K. Jondral, and M. Wintermantel, “Advances in automotive radar: A framework on computationally efficient high-resolution frequency estimation,” IEEE Signal Processing Magazine, vol.34, no.2, pp.36-46, 2017.
[4] D. A. Hague and J. R. Buck, “The generalized sinusoidal frequency-modulated waveform for active sonar,” IEEE Journal of Oceanic Engineering, vol.42, no.1, pp.109-123, 2017.
[5] Y. He, X. Shi, Y. Wang, and Y. Shen, “A fine frequency estimation algorithm based on DFT samples and fuzzy logic for a real sinusoid,” IET Radar, Sonar & Navigation, vol.16, no.8, pp.1364-1375, 2022.
[6] S. Ando, "Frequency-domain prony method for autoregressive model identification and sinusoidal parameter estimation," IEEE Trans.

Signal Process., vol. 68, pp. 3461-3470, 2020.

[7] F. Auger, P. Flandrin, et al., "Time-frequency reassignment and synchrosqueezing: An overview," IEEE Signal Process. Mag., vol. 30, no. 6, pp. 32-41, 2013.

[8] C. Candan, “A method for fine resolution frequency estimation from three DFT samples,” IEEE Signal Processing Letters, vol.18, no.6, pp.351-354, 2011

[9] E. Jacobsen, and P. Kootsookos, “Fast, accurate frequency estimators,” IEEE Signal Process. Mag., vol.24, no.3, pp.123-125, 2007.

[10] JR. Liao, and S. Lo, “Analytical solutions for frequency estimators by interpolation of DFT coefficients,” Signal Processing, vol.100, pp.93-100, 2014

[11] JR. Liao, and CM. Chen, “Phase correction of discrete Fourier transform coefficients to reduce frequency estimation bias of single tone complex sinusoid,” Signal Processing, vol.94, pp.108-117, 2014.

[12] E. Aboutanios, and B. Mulgrew, “Iterative frequency estimation by interpolation on Fourier coefficients,” IEEE Transactions on signal processing, vol.53, no.4, pp.1237-1242, 2005.

[13] Y. Chen, AHC. Ko, WS. Tam, CW. Kok, and Hc. So, “Non-iterative and accurate frequency estimation of a single cisoid using two DFT coefficients,” Digital Signal Processing, vol.98, no.7, pp.1-10, 2020.

[14] C. Candan, “Analysis and Further Improvement of Fine Resolution Frequency Estimation Method From Three DFT Samples,” IEEE Signal Process. Lett., vol.20, no.9, pp.913-916, 2013.

[15] ZL. Mou, YQ. Tu, P. Chen, and K. Wang, “Accurate frequency estimation of multiple complex and real sinusoids based on iterative interpolation,” Digital Signal Processing, vol.117, no.7, pp.1-12, 2021.

[16] U. Orguner, and C. Candan, “A fine-resolution frequency estimator using an arbitrary number of DFT coefficients,” Signal Processing, vol.105, pp.17-21, 2014.

[17] M.D. Macleod, “Fast nearly ML estimation of the parameters of real or complex single tones or resolved multiple tones,” IEEE Trans. Signal Process., vol.46, no.1, pp.141-148, 1998.

[18] D. Rife, and R. Boorstyn, “Single tone parameter estimation from discrete-time observations,” IEEE Trans. Inf. Theo., vol.20, no.5, pp.591-598, 1974.

[19] L. Cheng, W. Guo, C. Guo, and J. Zheng, “Performance analysis and evaluation of frequency-locked loop for weak GNSS signals based on spectral line interpolation,” IEEE Access, vol.8, pp.122396-122404, 2020.